240
2-25-77
UC-79b+d
Plus UK+ Germany + Japan

Dev. 739

AI-ERDA-13181

MASTER

TECHNICAL PROGRESS REPORT
FAST REACTOR FLUENCE DOSIMETRY
FOR PERIOD
JANUARY – NOVEMBER 1976

ERDA Research and Development Report

Prepared for the United States
Energy Research and Development Administration,
Division of Reactor Research and Development,
under Contract Number E(04-3)-824

EB

Rockwell International

Atomics International Division
8900 DeSoto Avenue
Canoga Park, California 91304

DISCLAIMER

Printed in the United States of America
Available from
National Technical Information Service
U.S. Department of Commerce
5285 Port Royal Road
Springfield, Virginia 22151
Price: Printed Copy $4.00 Microfiche $2.25

AI-ERDA-13181
LMFBR – FUELS AND MATERIALS
ENGINEERING AND DEVELOPMENT
UC-79b
LMFBR – PHYSICS
UC-79d

TECHNICAL PROGRESS REPORT
FAST REACTOR FLUENCE DOSIMETRY
FOR PERIOD
JANUARY – NOVEMBER 1976

The preceding Progress Report was AI-AEC-13167

Rockwell International
Atomics International Division
8900 DeSoto Avenue
Canoga Park, California 91304

CONTRACT: E(04-3)-824
ISSUED: December 23, 1976

DISTRIBUTION

This report has been distributed according to the categories LMFBR — Fuels and Materials Engineering and Development" and "LMFBR — Physics," as given in the Standard Distribution for Unclassified Scientific and Technical Reports, TID-4500.

CONTENTS

TABLES

FIGURES

THIS PAGE

WAS INTENTIONALLY

LEFT BLANK

Program:	LMFBR Technology				
ERDA Task:	2 - Fast Reactor Fluence Dosimetry				
Program Manager:	R. W. Keaten		**Project Manager:**	H. A. Morewitz	
Reporting Period:	January-November 1976		**Category:**	KG-07-00-00-0	
General Order:	06506	**Subaccount:**	29623	**189a Number:**	SA003

Principal Investigators: H. Farrar IV, R. A. Britten

I. PROJECT OBJECTIVES

The objectives of this task are to: (1) develop and demonstrate the use of ^{10}B and ^{6}Li helium accumulation fluence monitors (HAFM's) as a reliable and accurate method of measuring reactor neutron fluence; (2) develop and apply an expanded set of HAFM's which will provide fluence responses in different but overlapping neutron energy ranges; (3) identify, through the precise measurement of spectrum-integrated helium production cross sections, those elements which produce significant helium when used individually or as components of advanced alloys in FTR and LMFBR neutron environments, so that their use might be eliminated, minimized, or controlled; (4) use this information to predict, with confidence, the helium production rate for any alloy or material considered for fast reactor use, and (5) maintain a centralized helium measurements laboratory available to the research community, and upgrade the sample throughput capacity to handle FTR dosimetry requirements.

II. TECHNICAL PROGRESS DURING REPORT PERIOD

A. BACKGROUND AND SUMMARY

Accurate fluence and spectral characterization of very long experimental irradiations is required for adequate correlation of results and extrapolations to new FTR and LMFBR reactor environments. Accurate fluence information is equally important for the development of improved high performance materials.

To provide fluence-spectral data in addition to flux-spectral data, particularly for long-term irradiations, stable-product helium accumulation fluence monitors (HAFM's) are being developed to supplement current radiometric monitor reactions. The direct measurement of fluence is preferable to measuring flux and using the reactor power-time history, because total reactor power may not reflect local power at an experimental location, due to movement of control rods and changes in reactor loading.

A helium accumulation fluence monitor generally consists of a miniature capsule containing a known amount of material with a relatively high (n,α) cross section for the neutron spectrum of interest. The capsule itself is fabricated from a material with a low (n,α) cross section, so that when the whole HAFM is vaporized during the final analysis, the helium contribution from the capsule is small compared with that generated and released by the contents. Encapsulation is desirable not only to contain the material itself and any helium that might diffuse out of it, but also to prevent interaction of the contents with other nearby materials. Vanadium has been used for encapsulating ^{235}U, ^{237}Np, ^{238}U, and ^{239}Pu "fission foils" included in HEDL's multiple foil sets, and has also been selected to encapsulate HAFM's used in fast reactors, because of its low (n,α) cross section and low induced radioactivity.

The first HAFM's contained the isotopes ^{10}B and ^{6}Li. Numerous irradiations of these have been made in the Experimental Breeder Reactor-II (EBR-II) and in three low-power well-characterized test reactor environments. The latter irradiations are being used to normalize the spectrum integrated helium production cross sections of ^{10}B and ^{6}Li, providing increased accuracy for their use in fast reactor situations.

During FY 1976, the "multiple foil" technique employed by the Fast Reactor Materials Dosimetry Center at HEDL was expanded to include HAFM's containing ^{6}Li and ^{10}B. These HAFM's were included in routine flux-spectral sets during several B_4C experimental tests. The helium in these and in other HAFM's was measured with ~2% absolute accuracy by isotope dilution mass spectrometry. The results of another 30 HAFM's irradiated as a part of the Run 75D EBR-II dosimetry test have given important flux-spectral information for this test. It was

found that the ratio of the ^{10}B and ^{6}Li reaction rates is strongly dependent on $\bar{E}$, the mean energy of the neutron spectrum, demonstrating the value of these reactions as fluence-spectrum as well as total fluence monitors.

Irradiations of numerous ^{10}B and ^{6}Li specimens in the benchmark neutron spectra of the Coupled Fast Reactivity Measurements Facility (CFRMF) and BIG-10 facilities have provided important integral normalizations of the ^{10}B and ^{6}Li helium production cross sections. For fuels and materials experiments in EBR-II, FTR, and other fast and thermal test reactors, the use of these HAFM's is significantly increasing the accuracy of fluence measurements needed for the correlation and subsequent application of irradiation effects data.

Additional HAFM's containing materials with different (n,α) cross section energy responses are also being developed. Analyses have been started on the 300 that were irradiated at five core and blanket locations in EBR-II during the Run 75D dosimetry test. Expanded HAFM sets will provide a direct measure of the fluence-spectrum, instead of the usually-obtained flux-spectrum. By including different materials in the HAFM's, all neutron energy ranges important to LMFBR correlations will be covered.

Numerous helium concentration measurements have been made on both irradiated and unirradiated Type 316 stainless steel tubing that had been pressurized by helium at elevated temperatures. The results indicate that, without the presence of neutrons, helium penetrated a small distance into the tubing inner surfaces at elevated temperatures. In EBR-II irradiated tubing, however, a combination of helium pressure and the neutron environment resulted in a factor-of-ten greater helium concentration than neutrons alone or pressurization alone would have produced. These synergistic findings are relevant to recent AI-HEDL measurements of helium enhancements on inner layers of EBR-II fuel pin cladding. Further joint experiments are now being planned using existing irradiated tubes at HEDL to determine whether the neutron environment, in addition to affecting the helium concentration, also increases the depth of helium penetration.

TABLE 1

HELIUM CONCENTRATIONS IN HAFM'S CONTAINING NATURAL BORON IRRADIATED IN EBR-II RUN 75D DOSIMETRY TEST

HEDL Capsule Number	EBR-II Location			Mass of Natural Boron (mg)	Total Number of ^4He Atoms Measured	^4He Released by Puncture (%)	Helium Concentration* (ppm per ^{10}B)	
	Position	R (cm)	Z (cm)				^3He	^4He
6	4C3	17.3	-33.88	0.2082	1.679×10^{16}	-	0.85	7309
7	4C3	17.3	-20.78	0.1757	7.836×10^{15}	-	1.24	4038
8	4C3	17.3	-12.60	0.1865	5.434×10^{15}	8.6	0.43	2630
10	4C3	17.3	+13.22	0.1681	4.932×10^{15}	10.4	0.51	2648
11	4C3	17.3	+19.22	0.1419	5.252×10^{15}	-	-	3347
12	4C3	17.3	+39.43	0.2176	1.175×10^{16}	-	-	4893
13	4C3	17.3	+59.44	0.1895	9.265×10^{15}	-	-	4433
14	4E1	19.8	-0.80	0.1583	4.590×10^{15}	-	0.62	2609
16	4E1	19.8	+19.22	0.1461	4.974×10^{15}	-	0.21	3078
30	7F4	33.1	-0.71	0.1962†	6.851×10^{15}	9.2	0.21	3161
33	8F4	33.4	-14.62	0.1560†	6.383×10^{15}	15.3	-	3778
34	8F4	33.4	-0.06	0.2017†	7.327×10^{15}	11.0	-	3291
35	8F4	33.4	+13.47	0.1597†	5.706×10^{15}	11.6	-	3239
43	8F4	38.3	-0.61	0.1974†	7.853×10^{15}	7.8	-	3634

*Corrected for calculated number of helium atoms contributed by the vanadium (see text).
†After the HAFM capsule was punctured, the original B crystal was removed, reweighed and analyzed for ^4He without the vanadium.

B. HELIUM ACCUMULATION FLUENCE MONITORS

Final results for 14 helium accumulation fluence monitors (HAFM's) containing natural boron, and 15 containing enriched ^{6}LiF, are presented in Tables 1 and 2, respectively. All these HAFM's were irradiated in EBR-II as an integral part of HEDL's flux-spectral sets during the Run 75D dosimetry test. The results will become a part of the SAND-II Code flux-spectral characterization for EBR-II. The helium analyses of all the boron HAFM's were performed as part of this program; additional funding was provided by HEDL to complete the ^{6}LiF work.

1. Manufacture and Irradiation of HAFM's

All the HAFM's were manufactured in mid-1974 by the Isotope Target Center at ORNL. Individual crystals of natural boron and enriched ^{6}LiF were originally prepared at AI from single pieces of high-purity material. The isotopic content of the boron was determined at ORNL and HEDL to be 19.80% ^{10}B. The enrichment of the ^{6}LiF was determined at ORNL (99.164%), and at HEDL (99.038%) giving an average value of 99.10 ±0.09% ^{6}Li.

Each crystal was selected at AI under microscope for its lack of protrusions and its absence of visible flaws. Following this selection, the crystals were washed to remove dust and surface contamination, and were then placed in a high vacuum chamber to remove surface moisture and other gases. Each crystal was finally weighed with a 2σ uncertainty of <1% of the absolute mass value, using a substitution weighing scheme and standard weights traceable to the U.S. National Bureau of Standards.

At ORNL, each crystal was reweighed using a similar procedure, to ensure that none of the crystal had broken off. This weighing was followed by insertion into the miniature vanadium capsule (1.27 mm OD, 3.18 mm length) and final sealing by Tungsten Inert Gas (TIG) fusion welding. The mass values for the crystals listed in Tables 1 and 2 are the average values for the AI and ORNL weighings. Complete listings and comparisons of all the ^{6}LiF and boron crystal weighings made at AI and ORNL are in preparation. For the crystals in the

TABLE 2

HELIUM CONCENTRATIONS IN HAFM'S CONTAINING ENRICHED ^{6}LiF

HEDL Capsule Number	EBR-II Location			Mass of LiF (mg)	Number of ^{4}He Atoms Measured	Tritium Retained (%)	Helium Concentrations (appm) with Respect to ^{6}Li*	
	Position	R (cm)	Z (cm)				^{3}He	^{4}He
1	2D1	5.2	-0.1	0.1510	6.882×10^{15}	81	100.4	1889
5	4C3	17.3	-59.8	0.1597	5.937×10^{15}	78	78.8	1558
6	4C3	17.3	-33.6	0.3278	1.767×10^{16}	--	--	2259
7	4C3	17.3	-20.5	0.2882	1.129×10^{16}	66	39.4	1638
10	4C3	17.3	+13.9	0.1717	5.868×10^{15}	--	--	1421
14	4E1	19.8	-0.1	0.1529	5.889×10^{15}	--	--	1597
24	7F4	28.2	-0.7	0.1932	6.287×10^{15}	--	--	1354
30	7F4	33.1	-0.7	0.3077	1.009×10^{16}	94	83.3	1370
31	8F4	33.4	-60.7	0.1884	4.443×10^{15}	98	61.4	989
32	8F4	33.4	-40.6	0.2040	7.274×10^{15}	84	79.4	1495
33	8F4	33.4	-14.6	0.1510	5.158×10^{15}	85	80.5	1429
35	8F4	33.4	+13.5	0.1012	3.133×10^{15}	73	62.8	1294
36	8F4	33.4	+19.4	0.1812	5.505×10^{15}	72	60.4	1272
37	8F4	33.4	+39.3	0.1482	4.101×10^{15}	66	50.5	1160
38	8F4	33.4	+59.4	0.1939	3.960×10^{15}	60	33.9	856

*Corrected for calculated number of helium atoms contributed by the ^{51}V and ^{19}F (see text).

29 HAFM's reported here, however, the average difference between the mass values from the two laboratories was only 0.4 μg, which amounted to an average uncertainty of ~0.2%.

The capsules were irradiated in January 1975 during the full power EBR-II dosimetry test Run 75D. The locations of each of the HAFM's are given in Tables 1 and 2. Following the irradiation, the HAFM's were unloaded from the HEDL dosimetry capsules and shipped to AI for helium measurement. Identification was confirmed by weight and by using the dot code stamped on the capsule sides. Prior to being loaded into the mass spectrometer system's high temperature furnace, each HAFM was washed in warm H_2O with the aid of ultrasonic vibration, dried and weighed.

2. Special Measurements of the Retention of Helium by Boron Crystals

The majority of the HAFM's were analyzed for helium by vaporizing the capsules and their contents in the mass spectrometer high temperature furnace. Seven of the boron HAFM's listed in Table 1 underwent a special procedure to help in the understanding of the release of helium by the boron crystals themselves, and the retention of the helium by the vanadium capsule walls. Instead of vaporizing the HAFM capsules and their contents, the capsules were placed in a holder under high vacuum, the tops were sheared off, and the helium released was measured. Following this capsule penetration, five of the capsules were cut open and the submilligram crystals of boron were removed, reweighed, and then analyzed individually for helium content. The vanadium capsule walls may be studied later to determine the extent of helium penetration. The seventh column of Table 1 shows that between 9 and 16% of the total measured helium was released upon puncturing.

3. Study of Tritium Retention by the HAFM's

A slightly-modified mass spectrometric procedure was devised to allow, in some cases, the measurement of ^3He as well as the more important ^4He. This measurement is necessary in the case of ^6LiF because equal numbers of tritium and helium atoms are generated each time a $^6Li(n,\alpha)t$ reaction occurs, and the

tritium decays to ^{3}He with a half-life of 12.3 years. In the case of boron, the ^{3}He is generated by the decay of tritium formed by the high-energy threshold reaction $^{10}B(n,2\alpha)t$. Even though only ~6% of the tritium had decayed to ^{4}He at the time the HAFM's were analyzed, the amount of this isotope already in the sample must be known so that its contribution can be subtracted from the much larger ^{3}He spike later added for calibration purposes.

The measurement of the ^{3}He was accomplished by taking a small known fraction (0.13%) of the gas released from the vaporized HAFM capsule, before the ^{3}He spike was added. After the ^{3}He content was measured with respect to the ^{4}He, the ^{3}He spike was added to the remainder of the gas sample, and the altered isotopic ratio was measured to provide absolute concentration. Using this procedure, precise determinations were made of both ^{3}He and ^{4}He.

As can be seen from Table 1, the concentrations of ^{3}He were three to four orders of magnitude less than the ^{4}He. For ^{10}B, the uncertainties attached to the ^{3}He measurements range from 5 to 60%. These high uncertainties arise because the amount of ^{3}He present is small, and the mass spectrometer was operated in an insensitive mode optimized for the precise measurement of the more-abundant ^{4}He. Nevertheless, in all cases the amount of ^{3}He released by the boron HAFM's was found to be negligible compared to the ^{3}He calibration spike.

The last column of Table 2 gives the percentage of tritium retained in the ^{6}LiF HAFM capsules through the nine-day irradiation and the subsequent time period (~0.7 to 1.2 years). Since equal numbers of α-particles and tritium atoms are formed by the $^{6}Li(n,\alpha)t$ reaction, the retention of the tritium can be calculated from the ^{3}He and ^{4}He measurements if it is assumed that both the ^{3}He and ^{4}He were totally contained. It is interesting to note that for the 8F4 Position, the percentage of tritium that was retained dropped steadily from 98% at the -60.7 cm location (coolest) to 60% at the +59.4 cm location (hottest).

4. Routine Mass Spectrometer Procedures, Corrections, and Accuracies

Precise measurements of ^4He were made by adding known amounts of ^3He to the vacuum furnace enclosure either immediately before or after the vaporization of the HAFM. The ^3He spikes (~1.4×10^{16} atoms) were obtained by expanding and partitioning a known quantity of gas through a succession of calibrated volumes. The mass spectrometer was repeatedly calibrated for mass fractionation during each series of runs by analyzing known mixtures of ^3He and ^4He. Absolute uncertainty, determined from the cumulative uncertainties of sample weight, isotope ratio measurement, and spike size, is estimated to be <1.5% of the concentration value for this series of runs.

After measuring the total amount of helium released by vaporizing the HAFM vanadium capsule and its contents, it was necessary to calculate the contribution to the total coming from the vanadium itself. Since no empty vanadium capsules were irradiated with these HAFM's to give this information, the contribution was calculated using fluence data generated by multiple foils irradiated along with the HAFM's in adjacent capsules. The corrections for the vanadium contributions to the helium were always small, ranging from a maximum of 0.8% for core-center HAFM's to a minimum of <0.001% for blanket locations far from the core. Similar calculations were made for the small contributions to the helium production from the ^{19}F and ^7Li in the ^6LiF crystals. The corrections for ^{19}F ranged from a maximum of 0.5% to a minimum of less than 0.001%, and the ^7Li corrections were 100 times less than this. Uncertainties introduced by all these corrections were negligible.

The helium concentrations listed in Tables 1 and 2 were calculated relative to the number of ^{10}B or ^6Li atoms present. In the cases where no ^3He measurements were made before the spike was added, adjustments were made to the values of the added ^3He spikes using calculated values. The adjustments were small in every case, and the uncertainties arising from them were negligible compared to uncertainties arising from other sources.

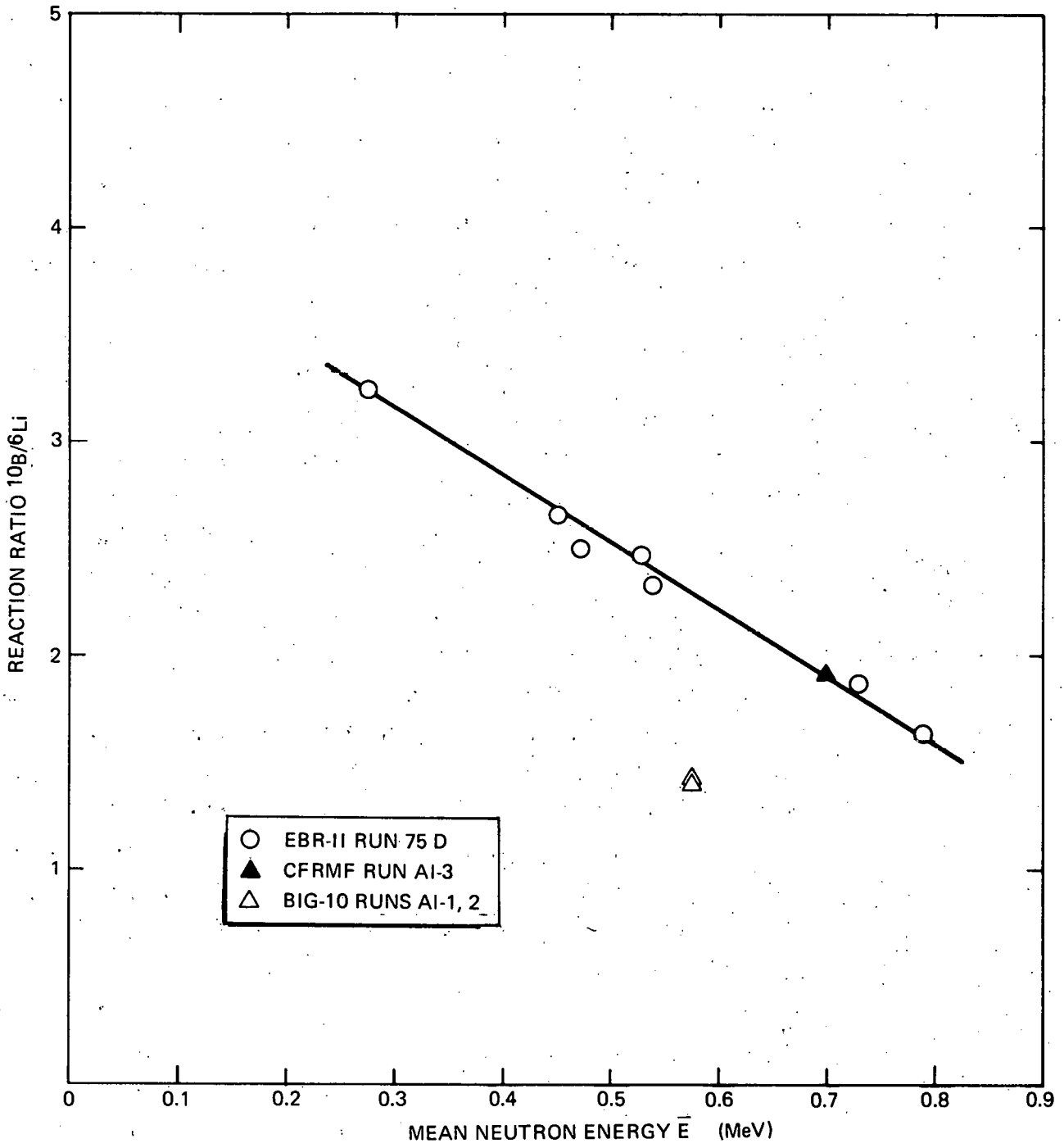

Figure 1. Comparison of ^{10}B and ^{6}Li Helium Accumulation Fluence Monitors Irradiated in EBR-II, CFRMF and BIG-10 with Preliminary SAND-II Calculated Neutron Mean Energy Values.

5. Energy Sensitivity Demonstrated by B and Li HAFM's

Table 3 lists the HEDL dosimetry capsules for which both boron and lithium HAFM's have been analysed. Of particular interest is the sixth column, which shows that the ratio of the reaction rates of ^{10}B and ^{6}Li varies between 1.63 and 3.24. The ratio is strongly dependent on location within the core and blanket regions, being lowest at midplane, and highest at the furthest-out location. The last columns in Table 3 shows values of the mean neutron energy ($\bar{E}$) calculated by HEDL based on preliminary SAND-II unfolded neutron spectra using flux-fluence information obtained during the same EBR-II irradiation.

TABLE 3
LOCATION AND ENERGY SENSITIVITY OF ^{10}B and ^{6}Li HAFM'S IN EBR-II

HEDL Capsule	EBR-II Location		Helium Concentration (appm)			$\bar{E}$ (MeV)
	R (cm)	Z (cm)	per ^{10}B	per ^{6}Li	$^{10}B/^{6}Li$	
6	17.3	-33.6	7309	2259	3.24	0.28
7	17.3	-20.5	4038	1638	2.47	0.53
10	17.3	+13.9	2648	1421	1.86	0.73
14	19.8	-0.1	2609	1597	1.63	0.79
30	33.1	-0.7	3161	1370	2.31	0.54
33	33.4	-14.6	3778	1429	2.64	0.45
35	33.4	+13.5	3239	1294	2.50	0.47

As expected, the ratio of the ^{10}B and ^{6}Li reaction rates is strongly dependent on $\bar{E}$, as shown in Figure 1. The remarkably close linear fit of the data demonstrates the value of these two HAFM types as total fluence and fluence-spectrum monitors.

Also plotted in Figure 1 are preliminary results from the benchmark facilities BIG-10 and CFRMF (see Section II.C). The CFRMF datum falls very well among the EBR-II data. Contrary to this and as expected, the data from the two BIG-10 irradiations fall far below the line because the neutron spectrum shape of this facility is much different from EBR-II and CFRMF below 40 keV, a region of importance to the ^{10}B and $^{6}Li(n,\alpha)$ cross sections. Simple correlations of the $^{10}B/^{6}Li$ ratio with $\bar{E}$ should be expected only for similar neutron spectrum compositions. In all cases, sophisticated unfolding techniques (SAND-II code) must be used to correlate the information properly.

C. TESTING OF B AND Li HAFM's IN STANDARD NEUTRON BENCHMARK FIELDS

As part of Atomics International's contribution to the Interlaboratory LMFBR Reaction Rate (ILRR) program, several irradiations of ^{10}B and ^{6}Li have been made in four separate standard neutron benchmark facilities. Numerous specimens from these irradiations have now been analyzed for helium, and the final measurements are reported here. Additional irradiations of B and Li in two benchmark spectra at NBS have been identified in the ILRR program plans. A further irradiation of other HAFM materials in the Coupled Fast Reactivity Measurements Facility (CFRMF), operated at higher power, is being considered.

The spectrum integrated cross section results of the measurements of the helium generated by the $^{10}B(n,\alpha)^{7}Li$ and $^{6}Li(n,\alpha)t$ reactions are now being used to normalize existing energy-dependent cross section data for LMFBR-type neutron spectra. These normalized cross sections, when computed, will provide increased fluence accuracy for ^{10}B and ^{6}Li helium accumulation fluence monitors (HAFM's) currently included in flux spectral sets in EBR-II, BR2 (Belgium), PFR (Scotland), and Rapsodie (France).

1. Irradiation Conditions

The first two irradiations of ^{10}B and ^{6}Li in the 1975-76 ILRR program series were conducted in the BIG-10 standard neutron field at the Los Alamos Scientific Laboratory. Two small aluminum assemblies were used to hold a

number of ^{10}B, natural B, and ^{6}LiF bare crystals, and 12 miniature capsules containing ^{10}B or ^{6}LiF crystalline powder. Each assembly was placed adjacent to the location of several other experiments conducted by participants of the ILRR program. After the first four identical ILRR program experimental irradiation cycles, the first AI assembly was removed and was replaced by an almost-identical second assembly for the five remaining cycles in the series.

The third irradiation of another identical aluminum assembly with the same contents took place by itself, for 30 hr at 6 kw in the CFRMF at the Idaho Nuclear Engineering Laboratory (INEL). The fourth and fifth irradiations were conducted especially for the B and Li HAFM's by the CEN/SCK Laboratories at Mol, Belgium, in the Sigma Sigma ($\Sigma\Sigma$) and Fission Cavity ($\pi\Sigma$) benchmark fields of the BR1 reactor.

2. Measured Concentrations of Helium

The measured results of 36 helium analyses of the enriched ^{6}LiF, natural boron, and enriched ^{10}B crystals irradiated in BIG-10 (2 runs) and CFRMF are presented in the fifth and sixth columns of Tables 4 and 5. Three ~6 mg ^{6}LiF crystals were included in each of the three irradiations. As a result of the irradiations, these crystals contained enough helium (>4 atomic parts per billion ^{4}He) that each could be split into two (labeled A and B) for accurate duplicate analysis. This splitting provided an opportunity to measure, in addition to the important ^{4}He content, the ^{3}He content accumulated from decaying tritium also produced as a result of the (n,α) reaction. In order to measure the ^{3}He, however, no ^{3}He calibration spike could be added during the analysis, and the absolute ^{3}He and ^{4}He contents were determined (with slightly less accuracy) by careful comparison of mass spectrometer response before and after the analysis.

3. Self-Shielding and Flux Depression Calculations

The last column of Tables 4 and 5 present the helium concentration data with preliminary small corrections made for neutron self-shielding by the

TABLE 4

HELIUM GENERATED IN ^{6}LiF CRYSTALS BY BENCHMARK IRRADIATIONS

Irradiation Facility	Sample Number	Sample Mass (mg)	Number of ^{4}He Atoms Released	Helium Concentration With Respect to ^{6}Li (appb)		
				^{3}He	^{4}He (Measured)	^{4}He (corrected)††
BIG-10 (AI Run 1)	R6LiF1A	3.0941	3.048×10^{11}	0.396	4.13*	4.17*
	R6LiF1B	3.1794	3.138×10^{11}	--	4.14	4.18
	R6LiF2	4.9174	4.904×10^{11}	--	4.18†	4.22
	R6LiF4	3.9503	3.860×10^{11}	0.425	4.10*	4.14*
BIG-10 (AI Run 2)	R6LiF3A	2.8749	3.674×10^{11}	0.462	5.36*	5.42*
	R6LiF3B	2.4646	3.058×10^{11}	--	5.20	5.26
	R6LiF5	4.5287	5.660×10^{11}	0.474	5.24*†	5.30*
	R6LiF13A	3.3402	4.118×10^{11}	--	5.17	5.23
	R6LiF13B	3.2086	3.946×10^{11}	--	5.16	5.22
CFRMF (AI Run 3)	R6LiF9A	2.8710	5.607×10^{11}	0.380	8.19*	8.23*
	R6LiF9B	2.6647	5.124×10^{11}	--	8.06	8.10
	R6LiF11	4.4658	8.536×10^{11}	--	8.01†	8.05
	R6LiF14A	3.3223	6.338×10^{11}	--	8.00	8.04
	R6LiF14B	2.1641	4.146×10^{11}	0.411	8.03*	8.07*

*Six samples were analyzed for ^{3}He as well as ^{4}He, resulting in a slight loss of absolute accuracy.

†Three samples were etched to remove surface LiF which is expected to have lost some helium by α-recoil.

††Measured values have been adjusted for neutron self-shielding and flux depression using preliminary calculations, and for the small contribution to the total helium generated by ^{19}F.

TABLE 5

HELIUM GENERATED IN BORON SAMPLES BY BENCHMARK IRRADIATIONS

Irradiation Facility	^{10}B Isotopic Enrichment	Sample Number	Sample Mass (mg)	Number of ^{4}He Atoms Released	^{4}He Concentration With Respect to ^{10}B (appb)	
					Measured Values	Corrected Values††
BIG-10 (AI Run 1)	19.80	RNB5	2.9438	1.924×10^{11}	5.926	5.998
	19.80	RNB6E	3.8439	2.503×10^{11}	5.904†	5.976
	19.80	RNB12	4.0066	2.610×10^{11}	5.906	5.978
	95.6	R10B1	3.6106	1.201×10^{12}	5.810	5.910
	93.0	R10B41	2.3555	7.612×10^{11}	5.817	5.918
	93.0	R10B42	1.5856	5.176×10^{11}	5.875	5.977
BIG-10 (AI Run 2)	19.80	RNB7	4.4364	3.676×10^{11}	7.512	7.603
	19.80	RNB8E	3.9819	3.284×10^{11}	7.476†	7.567
	19.80	RNB9	3.6992	3.002×10^{11}	7.358	7.447
	19.80	RNB14E	3.3432	2.764×10^{11}	7.497†	7.588
	95.6	R10B3	3.5012	1.459×10^{12}	7.281	7.407
	93.0	R10B44	1.8901	7.675×10^{11}	7.308	7.434
	93.0	R10B45	1.8184	7.342×10^{11}	7.267	7.393
	93.0	R10B48E	1.9120	7.799×10^{11}	7.342†	7.469
CFRMF (AI Run 3)	19.80	RNB11E	5.5537	9.484×10^{11}	15.47†	15.61
	19.80	RNB13	4.3437	7.411×10^{11}	15.47	15.60
	19.80	RNB15	4.7799	8.120×10^{11}	15.40	15.54
	19.80	RNB16E	5.3543	9.183×10^{11}	15.55†	15.69
	95.6	R10B18	2.7334	2.309×10^{12}	14.76	15.23
	93.0	R10B47	1.4514	1.182×10^{12}	14.66	15.10
	93.0	R10B49E	1.9070	1.577×10^{12}	14.88†	15.32
	93.0	R10B50	1.7381	$\sim 1.44 \times 10^{12}$	~14.88*	~15.32*

*Sample R10B50 was also analyzed for ^{3}He (0.0003 appb), resulting in a slight loss of absolute accuracy in the ^{4}He measurement.

†Seven samples were etched to different known degrees, to remove surface boron expected to have lost helium by α-recoil, and to measure neutron self-shielding.

††Measured values have been adjusted for neutron self-shielding and flux depression using preliminary calculations (see text).

crystals, and for flux depression caused by the presence of the whole irradiation package. The listed helium concentration levels are those that would have accumulated in an infinitesimally small sample had there been no AI irradiation package or nearby fission chamber present during the irradiation. The flux depression and self-shielding corrections were calculated by G. E. Hansen (LASL) for the BIG-10 irradiations, and by E. P. Lippincott (HEDL) for CFRMF. In the case of the BIG-10 irradiations, the corrections range from 1.2% for natural boron, to 1.7% for enriched ^{10}B. In the case of the CFRMF run, the corrections ranged from 1.0% (for ^{6}LiF) to 3.2% (for the biggest crystals of enriched ^{10}B). Unlike the BIG-10 case, however, no correction is included for flux depression by the irradiation chamber walls. Since the chamber was present during all the reactor runs, whether or not this correction is made has little effect on the final results, as long as it is used consistently for all the different ILRR program test experiments in that reactor.

Examination of the measured data in Table 5 shows that the higher enrichments of ^{10}B did have lower helium concentrations, but the self-shielding corrections do not bring the data into complete agreement with the natural boron (19.8% ^{10}B) data. For CFRMF, where the discrepancy is larger, calculations indicate there should have been a 2.2% difference between the enriched ^{10}B and the measured natural boron results due to self-shielding. In actual fact, the measured difference was 4.8%; and as a result, there is still a 2.6% difference between the ^{10}B and natural boron data after the self-shielding corrections have been made. For the BIG-10 results, the residual difference in the self-shielding-corrected results is only 1.3%.

To help study the self-shielding phenomenon, three of the ^{6}LiF crystals and seven of the boron crystals were etched to remove a surface layer, prior to helium analysis. The removed outer layer is expected to have been slightly depleted in helium due to α-recoil. The remaining material, however, representing the interior part of the crystal, is known to have experienced greater neutron self-shielding. A comparison of the helium concentration in the etched samples with the unetched samples therefore provided information on both phenomena, which both decrease the measured helium. The results in Tables 4

and 5 show that the etched samples have very similar helium concentrations; being on the average, only 0.6% higher than the unetched specimens. Efforts must be made to improve the self-shielding and α-recoil correction calculations, before reporting final helium generation results.

Small additional corrections to the ^{6}LiF results were made to account for the helium generated by the ^{19}F. For the BIG-10 irradiations, SAND-II code corrections calculated by E. P. Lippincott (HEDL) amounted to only 0.36%, and for CFRMF, to 0.52%. A correction for the helium generated by the ^{7}Li in the 99.1% enriched ^{6}LiF was negligible.

4. Reactions per ^{10}B and ^{6}Li Nucleus

Despite the small uncertainties remaining in the self-shielding and α-recoil corrections, the results in the final columns of Tables 4 and 5 are in excellent agreement. The weighted average values for the numbers of reactions per ^{10}B nucleus are $(5.960 \pm 0.036) \times 10^{-9}$, $(7.489 \pm 0.085) \times 10^{-9}$ and $(15.44 \pm 0.22) \times 10^{-9}$ for the BIG-10 Run 1, BIG-10 Run 2 and CFRMF Run 3 irradiations, respectively. The equivalent weighted average values for ^{6}Li are, respectively: $(4.195 \pm 0.028) \times 10^{-9}$, $(5.249 \pm 0.054) \times 10^{-9}$ and $(8.075 \pm 0.051) \times 10^{-9}$ reactions per ^{6}Li nucleus. From these data, the ratios of the reactions (or spectrum integrated helium production cross sections) for ^{10}B and ^{6}Li are 1.424 ± 0.004 for BIG-10, and 1.912 ± 0.012 for CFRMF. These ratios are plotted in Figure 1 versus $\bar{E}$, the mean neutron energy, for comparison with the EBR-II HAFM data described in Section II.B of this report.

Important correlations of these numbers with the measured fission rate of ^{235}U and with the detailed neutron spectra obtained for these benchmark reactors will be included in a future report. At this time it can be said, however, that the CFRMF results for ^{10}B with respect to ^{235}U are very close to those published earlier by this laboratory.*

*"Helium Production Cross Section of Boron for Fast-Reactor Neutron Spectra," by H. Farrar IV, W. N. McElroy, and E. P. Lippincott, Nucl. Tech. 25 305 (1975).

5. Estimated Uncertainties

The measured values of helium concentration listed in Tables 4 and 5 have an estimated absolute 1σ uncertainty of 1%. The final weighted average values have a relative uncertainty of better than 0.6%. These uncertainty levels are supported by the fact that the average helium production levels for ^{6}Li and ^{10}B are proportional to the total neutron fluences, for the two BIG-10 irradiations, to within 0.2% for ^{6}Li and to within 0.6% for ^{10}B.

Although some further corrections for self-shielding and α-recoil must still be made, they are expected to change the results very little. Also, since the corrections will be applied both to the boron and lithium fluoride results, the changes are expected to have an even smaller effect on the quoted $^{10}B/^{6}Li$ reaction ratios.

6. Vanadium Capsules Irradiated in BIG-10 and CFRMF

Twelve miniature capsules containing ^{10}B and ^{6}LiF crystalline powder made up the bulk of the material that was included by AI in each of the BIG-10 and CFRMF irradiations. The purpose of the encapsulation was to prevent loss of helium from the materials in the unlikely event that helium would diffuse significantly at the ambient temperatures of the irradiations.

Prior to analyzing the irradiated capsules, four unirradiated capsules from the same manufactured lots were routinely analyzed for helium to determine instrument background under the same analysis conditions. Unexpectedly, all four capsules (two containing ^{6}LiF, one with ^{10}B, and one empty) released helium in quantities ranging from 3×10^{10} to 3×10^{12} atoms, where no detectable amounts were expected. Such levels of helium would be of little consequence to HAFM's irradiated in EBR-II, where 10^{15} atoms of ^{4}He are usually generated (see Section II.B), but are very important to the low-level benchmark tests for which the capsules were intended. In fact, no more than 1 to 3×10^{12} atoms of ^{4}He were expected to have been generated in each capsule by the BIG-10 and CFRMF irradiations.

Investigations were then made into the source of the helium in the unirradiated capsules. It was already known that the ^{6}LiF and ^{10}B crystalline materials had little, if any, helium initially. Subsequent analyses of single crystals of ^{10}B and ^{6}LiF revealed undetectable levels. In order to remove any possible helium from the boron, moreover, the original batch had been melted under vacuum using an electron beam furnace. Although specifications indicated that helium could not be used during any step of the processing, it was subsequently found that the vanadium used to manufacture the HAFM capsules had come from two lots, one of which had been treated with argon, but the other had been arc-melted under one atmosphere of helium.

The net result of this helium/argon processing difficulty is that none of the special vanadium HAFM capsules manufactured in 1974 specifically for testing in benchmark facilities, may be used for low-level fluence irradiations. As mentioned earlier, these low-levels of helium within the vanadium material are negligible compared with the helium generated by the ^{10}B and ^{6}Li in EBR-II irradiations. Nevertheless, the planned studies of helium diffusion through the walls of EBR-II irradiated HAFM's will be discontinued because the measurements would be confused by the helium already within the walls.

7. Tritium Determined by ^{3}He Buildup

The measured ^{3}He data in the six ^{6}LiF samples analyzed for this isotope were compared with the computed ^{3}He that decayed from tritium produced as a result of the $^{6}Li(n,\alpha)t$ reaction. The results show that the $^{3}He/^{4}He$ ratio was equal to the expected value to within the ~10% uncertainties of the measurement of ^{3}He in the 4×10^{-10} atom fraction regime.

8. Discussion of Helium Diffusion

Even though the capsules included in the benchmark irradiations could not be used, there is evidence indicating that the bare crystals lost negligible amounts of helium, and that therefore encapsulation was unnecessary. First, the comparisons of encapsulated and unencapsulated boron specimens in an earlier

CFRMF irradiation indicated encapsulation was unnecessary. The possibility of loss of helium from the bare crystals due to diffusion is thought to be unlikely because the air surrounding the crystals already contains a helium concentration greater, in several cases, than that generated within the crystals. In-leakage from the air into unirradiated crystals has, moreover, been determined by measurements to be nonexistent. Furthermore, the concentrations of ^{3}He in the ^{6}LiF crystals are consistent with the concentrations of ^{4}He. That is, the results indicate that the ^{3}He is, within uncertainties, what would be expected if all the tritium and all the helium formed simultaneously by the $^{6}Li(n,\alpha)t$ reaction had been retained in the crystals. If there had been any diffusion of either, it might be expected that the loss would be quite different for helium than it would be for isotopes of hydrogen.

D. HELIUM ACCUMULATION FLUENCE MONITORS FOR LOW FLUENCE APPLICATIONS

One hundred eleven miniature stainless steel helium accumulation fluence monitor (HAFM) capsules containing enriched ^{10}B and ^{6}LiF crystals have been prepared for use in LMFBR and CTR neutron environmental characterization studies. These capsules were made at Atomics International both for this program and for a companion ERDA - Division of Magnetic Fusion Energy program, "Helium Generation in Fusion Reactor Materials," to characterize fast reactor neutron spectra for very low fluence situations. The capsules were made considerably larger than those currently used in operating fast reactors, and the amount of boron or lithium fluoride was maximized rather than minimized, to provide an optimum amount of helium for precise measurements. The ^{10}B and ^{6}LiF capsules contained, respectively, ~54 and ~16 mg of the isotopes ^{10}B and ^{6}Li.

In order to generate enough helium ($\sim 10^{11}$ atoms ^{4}He) for precise (~1-2% 1σ) measurements, an LMFBR spectrum neutron fluence of only 2 to 7 x 10^{13} neutrons/cm^2 is required. Even fluence levels of only 2 to 7 x 10^{12} neutrons/cm^2 will give less than 10% uncertainties in the measured ^{10}B and ^{6}Li reaction rates. This makes these HAFM's useful for flux/fluence-spectrum measurements in low-power mockup facilities such as the Engineering Critical Mockup (ECM) and the Zero Power Plutonium Reactor (ZPPR).

The impetus for manufacturing the low-fluence ^{10}B and ^{6}LiF HAFM's was the special benchmark irradiation provided by CEN/SCK (Mol, Belgium) as a part of the ILRR program. Details of this experiment were worked out by personnel from AI, HEDL and CEN/SCK during a visit to Belgium in September 1975. The simultaneous 100-hour irradiations of 30 of these HAFM's that took place in the Fission Cavity ($\pi\Sigma$) and the very well-characterized Sigma Sigma ($\Sigma\Sigma$) facility of the BR1 reactor will provide important (n,α) cross section verification for these two standard isotopes. The fact that all the HAFM's were manufactured in a single batch will maximize the accuracies of future experimental comparisons between other fast neutron environments and the $\Sigma\Sigma$ and Fission Cavity standard neutron fields.

E. PENETRATION OF HELIUM INTO TYPE 316 STAINLESS STEEL

1. Helium Profiles in Fueled Cladding

Experiments described in the previous semi-annual report (AI-ERDA-13167) revealed a significant enhancement of helium on the inner surfaces of fueled cladding. To better understand these findings, additional cladding samples were prepared and analyzed for helium under a contract with HEDL. Specimens of tubing were manufactured from N-lot prototypic FFTF 20% cold-worked Type 316 stainless steel, and were irradiated in EBR-II as a part of the FFTF Driver Fuel Development Program at HEDL*. The samples were selected by C. W. Hunter and G. D. Johnson (HEDL) from different fuel pins to examine the effects of axial location in the pin, and the effects of fuel and cladding composition. Ring samples were taken from nearby locations at the bottom of a fuel column. One was adjacent to enriched fuel, a second was next to the depleted uranium insulator, and a third was adjacent to the Inconel-600 reflector. Other cladding rings were selected for other variables including variations in nitrogen and boron composition, and differences in clad temperature. In each case, the ring of cladding was cut into ~10 layers using a lathe in a HEDL hot

*J. E. Hanson and W. E. Roake, "FTR Driver Fuel Development Program Status," in Proc. ANS Fast Reactor Fuel Element Technology, pp 497-515 (April 1971).

cell to permit measurements of the helium profiles across the wall thicknesses. For each ring, samples representing the full thickness were also prepared to provide the helium concentrations averaged over the full wall of the cladding.

Six cladding rings were cut into a total of 66 layers, each consisting of several submilligram size turnings. For each layer, the turnings were washed in warm water with ultrasonic vibration. Two pieces were then selected under optical microscope for uniformity of thickness and clean appearance, and were weighed in preparation for mass spectrometric helium analysis. Over one hundred of these specimens, representing the locations of greatest interest, were analyzed for helium. Additional specimens of Type 316 stainless steel wire wrap from the same cladding locations were first counted radiometrically to determine the $^{54}Fe(n,p)^{54}Mn$ reaction, and were then analyzed for their helium concentrations. Details of these findings will appear in a HEDL annual report.

The results of all these experiments showed that a considerable enhancement (more than a factor of two) of helium occurred in the first one or two mils of the inside cladding surface. These results are consistent with those reported in this program's previous semi-annual report. A surprising new find, however, is that a large helium gradient occurred at a location well below the fuel column, next to the Inconel-600 reflector. Helium concentrations of up to 50 appm were measured in samples taken from the innermost 0.3 mils of cladding at this location. This is over 11 times greater than that predicted and that measured in central and outer regions of the cladding at the same axial location. The particularly high concentration is undoubtedly due in part to the probability that this sample was an extra-thin inner surface layer. At this location, however, the direct implantation of helium from the fission process (ternary fission), which was the first postulated explanation for the enhancements, could not have occurred. A probable explanation, given the new results, is that helium is buried in the surface by elastic neutron collisions with the pin helium. It is then possible that further permeation into the cladding is enhanced by neutron displacement mechanisms. These mechanisms will be discussed in Sections II.E.4, after other relevant experimental data have been presented.

2. Penetration of Pressurized Helium into Unfueled Irradiated 316 SS

The results of helium analyses made on this program using N-2 Lot, 20% cold-worked Type 316 stainless steel pressurized creep tubing supplied by E. R. Gilbert from HEDL's Stressed Cladding Irradiation Experiment are presented in Table 6. The first four samples were irradiated with static sodium on each side of the tubing wall at various locations and temperatures in EBR-II Subassembly X157-X157A. The fifth sample (GE) was irradiated at a nearby location, and at the same time as Sample CM, but it consisted of a sealed tube containing helium pressurized to 1780 psi at reactor temperature. It is evident from the results in Table 6 that the presence of pressurized helium resulted in a factor of ten increase in the helium concentration in the wall, when averaged over the full tubing thickness from which the samples were taken.

TABLE 6

HELIUM IN PRESSURIZED AND UNPRESSURIZED TYPE 316 SS IRRADIATED TUBING FROM S/A X157

Sample Number	Mass (mg)	Location		Neutron Fluence ($n/cm^2 \times 10^{-22}$)		$\bar{E}$ (MeV)	T (^oC)	Helium Concentration (appm)	
		R (cm)	Z (cm)	Total	>0.1 MeV			Measured Values	Weighted Average
CR-A	1.1254	17.7	-28.6	0.19	0.13	0.38	377 ±6	0.160	0.161
B	1.4451							~0.18	±0.001
C	2.4565							0.161	
EV-A	1.0321	17.7	-28.6	0.77	0.5	0.38	377 ±6	0.718	0.715
B	1.3496							0.713	±0.003
DK-A	0.8503	17.7	+3.81	1.84	1.6	0.78	577 ±28	3.13	3.14
B	1.0994							3.15	±0.01
CM-A	1.5075	17.7	+3.81	0.45	0.40	0.78	577 ±28	0.774	0.769
B	1.0790							0.765	±0.006
GE*-A	1.2407	14.3	+3.81	0.49	0.43	0.78	577 ±28	8.43	7.85
B	1.4577							7.15	±0.65
C	0.9012							7.98	

*Sample GE was irradiated under very similar conditions to Sample CM but had an internal helium pressure of 1780 psi.

The measurements on fueled cladding, as discussed earlier in Section II.E.1, where steep helium gradients were observed on the inner surfaces of the cladding adjacent to the plenum gas, would suggest that much of the additional helium in this unfueled pressurized tube might be within a layer close to the inner surface. This helium was nevertheless buried within the material because the tubing specimens were cleaned for two minutes in concentrated nitric acid, and were stored under high vacuum for several hours before they were analyzed for helium. Multiple analyses of the specimens confirmed the findings in Table 6, providing a reproducibility of 0.5% for this series of runs. Absolute accuracy of any individual helium measurement is estimated to be better than 2% of the concentration value.

An additional outcome of those results in Table 6 where no helium pressurization occurs shows that, as expected, the correlation of helium concentration with fluence >0.1 MeV is better than the correlation with total neutron fluence. Additional calculations indicate that the helium concentration is in closer proportion to neutron fluence >1 MeV, in conformity with the knowledge that most of the helium generated by (n,α) reactions within the steel results from neutrons above this energy.

3. Penetration of Pressurized Helium into Unirradiated 316 SS

Two cylindrical tubes of prototypic Type 316 stainless steel were filled with helium to give 2000 psi pressure at test temperature. These tubes were then heated by E. R. Gilbert (HEDL) for 600 hours in an argon-filled oven; Capsule BC at 570°C (1055°F) and Capsule HF at 760°C (1400°F). The cylinders were pierced after this high-temperature bake, but only the lower temperature capsule (BC) gave an audible release of helium. This latter fact is consistent with the HEDL observation that Capsule HF ceased increasing in diameter after 300 hr testing, and is presumed to have lost its pressurization at that time.

Helium measurements were conducted on sections of the 0.015 in. thick walls of both capsules. When helium was found in the wall of the lower temperature (570°C) Capsule BC (even though no neutron irradiation had occurred), further

pieces of tubing were prepared using a lathe so that a profile of helium at various radial locations could be obtained. In addition to these samples, a single piece of the same lot of stainless steel that was completely enclosed within the higher temperature (760°C) Capsule HF was also analyzed for helium. In this case, the pressurized helium bathed both sides of the metal, at least for the first 300 hr before loss of pressurization. Helium measurements of the interior of this piece were made by analyzing the ~5 mil thick piece remaining after filing off the outer 5 mils on each side.

The results of the helium analyses are given in Table 7, where it can be seen that significant amounts of helium were measured only in the lower temperature Capsule BC. By analyzing only the innermost 1.5 mil surface, a helium concentration of 6.18 appm was measured, whereas the central and outermost layers contained only ~0.001 appm. Two "full thickness" specimens of Capsule BC tubing gave helium concentrations (averaged over the wall thickness) of 0.950 and 1.011 appm, in close agreement with each other. From the data in Table 7, it can be deduced that no significant amounts of helium penetrated Capsule BC walls by as much as 4 mils. Furthermore, all the Capsule BC data can be explained satisfactorily only if all or nearly all of the helium was present somewhere within the innermost 1.5 mil layer.

The results of Capsule HF are presumably complicated by the apparent loss of pressurization halfway through the 600 hour heating cycle. Helium was measured in all specimens analyzed, but at levels below 0.001 appm on the inner surfaces, and 0.002 to 0.004 appm on the outer surfaces. The single piece of steel that was enclosed within the capsule definitely still retained a helium concentration of ~0.87 appm, although the efforts to determine whether it was on the surface or in the interior provided conflicting data. It should be noted than an unirradiated, unheated archive sample contained less than 50 parts per trillion helium.

TABLE 7

HELIUM IN UNIRRADIATED PRESSURIZED TYPE 316 STAINLESS STEEL TUBES

Disposition of Pressurized Helium	Radial Location on Tubing From Which Sample was Taken	Helium Concentration (appm)	
		Capsule BC (570°C for 600 h)	Capsule HF* (760°C for 600 h)
2000 psi helium on inside of tubing only	Innermost 0.0015 inch	6.18	—
	Innermost 0.004 inch	2.36	0.00085
	Innermost 0.008 inch	1.65	0.00051
	Central 0.008 inch	0.0012	0.00001
	Outermost 0.008 inch	0.00015	0.0024
	Outermost 0.004 inch	0.0010	0.0033
	Total thickness of wall	0.980	0.0029
2000 psi helium on inside and outside	Outermost 0.005 inch	—	0.027
	Central 0.005 inch	—	0.0001
	Total thickness of wall	—	0.866
No helium on either side	Unheated archive piece	—	0.0000

* At approximately 300 hours, Capsule HF is believed to have lost its pressurization.

4. Explanations for the Helium Penetration Phenomenon

Several mechanisms were originally proposed when early measurements showed enhanced helium concentrations on the inner surfaces of fueled cladding:

1) (n,α) Reactions. The bulk of the helium is produced uniformly within the cladding walls by (n,α) reactions with the elements comprising the stainless steel. Certain elements with relatively high (n,α) cross sections in fast reactor neutron spectra such as Li, B, and N, might migrate to the cladding inner surfaces, from within the steel or from other locations up or down the fuel pin. A concentration of one or more of these elements would result in localized helium enhancement.

2) Ternary Fission. Helium is generated directly by the fission process (ternary fission). This mechanism produces α-particles with enough energy to penetrate cladding adjacent to the fuel by as much as ~2 mils.

3) Elastic Scattering of Pin Helium. Helium that exists between the fuel and the cladding, and in the plenum above the fuel, penetrates a small distance into the stainless steel as a result of elastic collisions with energetic neutrons. The depth of helium penetration by this mechanism is typically 0.1 to 0.3 mils.

4) Fuel α-Decay. Alpha decay of plutonium isotopes, whether in reactor or in storage, will deposit helium in the cladding.

5) Neutron-Enhanced Permeation. Once the helium is buried in the surface (by any of the above mechanisms), further movement is enhanced by neutron induced displacements of atoms in the cladding.

The combination of measured helium generation rates (or (n,α) cross sections) in pure elements, and fluences estimated from dosimetry test irradiations, satisfactorily explains the helium concentrations measured in the central and

outer regions of the cladding wall thickness. To explain the helium enhancements by Mechanism (1), however, would require surface concentrations of the impurities that seem unrealistically high.

The ternary fission process qualitatively explains the enhanced helium levels of cladding surfaces adjacent to fuel, but cannot contribute to the helium enhancements at the locations below the fuel column.

Observations relevant to Mechanism (3) were supplied by the results given earlier in Tables 6 and 7. A comparison of the helium penetration into stainless steel, with and without the presence of a neutron field, can be made using Samples CM and GE from Table 6, and Sample BC from Table 7. All were baked for 600 hours at 570^{o}C, but CM had no helium pressurization and BC had no neutron flux. It is apparent that the reactor environment, when combined synergistically with the presence of pressurized helium, resulted in a very much greater helium concentration (7.85 appm) than neutrons alone (0.77 appm), or pressurization alone (0.98 appm), would have produced.

Approximate calculations using Mechanism (3) indicate that neutron collisions with pin helium will easily explain the synergistic effects measured in both the fueled and unfueled EBR-II irradiated tubings, to the extent of the total number of helium atoms that would be added to the inner surfaces. The small penetration depth is not enough, however, to explain the ~3 mil penetrations measured in the EBR-II fueled cladding.

The possibility that fuel α-decay contributes significant quantities of helium was ruled out by calculations made by F. A. Garner (HEDL) earlier this year.

At this time, no sophisticated calculations have been made to see if neutron induced displacement mechanisms can explain the measured helium penetrations.

In the case of the fueled cladding, it is certain that all five mechanisms are contributing to the measured helium profile. It is the relative contributions that must be determined so that predictions of the long-term effects can be made. Although the presence of quantities of helium on the inner surfaces of irradiated tubing is of little consequence in itself, the fact that this phenomenon is greatly enhanced by the combination of neutron flux and helium pressure is much more significant. This is particularly important because both of these situations occur in LMFBR fuel cladding. Ternary fission certainly occurs; but the fission yield of ^{4}He is uncertain and so the magnitude of the contribution to the profile is not well defined. The proposed elastic scattering mechanism will be important only while some helium remains in the gap between the fuel and the cladding. As this gap closes, the plenum helium will be excluded, removing any further scattering contribution. Further helium movement, enhanced by the neutron flux, will continue, independent of the original implantation mechanism.

5. Further Investigations

All the above findings were discussed during a visit by AI personnel to HEDL in mid-September 1976. At that time, further joint AI-HEDL efforts were outlined to clarify the contributing phenomena. It was proposed that further helium measurements on existing irradiated and unirradiated helium-pressurized tubes that have undergone longer exposures should be undertaken. In particular, the helium gradient across a pressurized irradiated tube should be measured for both short and long EBR-II irradiation exposures. This will provide important information on whether a radiation-enhanced helium permeation phenomenon, in addition to affecting the helium concentration, also increases the depth of helium penetration as a function of neutron exposure.

F. HELIUM IN BELGIAN CLADDING IRRADIATED IN BR2

As a part of a series of interlaboratory agreements between AI, HEDL, and the CEN/SCK laboratories at Mol, Belgium, Atomics International performed helium analyses on five austenitic stainless steel cladding rings irradiated as

a part of the CEN/SCK fast reactor program. Details of the cooperative experiment were worked out at a meeting at Mol on September 18-19, 1975.

Five 6mm OD rings made from the austenitic stainless steel alloys 12R72HV, WN4981, and WN4970 were irradiated in the MFBS-6 cadmium-screened loop in the thermal high power reactor BR2 at Mol. At AI, each ring was sectioned to provide specimens with optimum size, and four of these were then selected to give a helium concentration profile around the ring perimeter. The results showed helium concentrations and, therefore, fast flux trends, with variations about the mean ranging from 0.9 to ~8%, depending on the cladding ring. Complete details are given in Atomics International Letter 76AT-2267 from H. Farrar IV (AI) to J. Debrue (Mol) dated April 5, 1976.

An additional specimen from each ring was etched extensively in warm aqua regia before being weighed and analyzed for helium content. Three of the five etched specimens showed a measurably lower helium concentration, indicating that one or both of the surfaces that had been etched away had an enhanced helium level. By comparing the helium in the etched specimens with an interpolated value from nearby unetched specimens, it was concluded that surface or near-surface helium was responsible for between 3 to 8% of the total helium in the as-received rings. It is clear that this surface enhancement could be quite significant for a thin surface layer, but when it was averaged with the helium in the full thickness ring, the increase from the surface contribution amounted to only a few percent.

G. MASS SPECTROMETER SYSTEM

The mass spectrometer system was maintained under ultra-high vacuum conditions, and was made available to other laboratories to perform ERDA-approved helium analyses. Separate contracts in FY 1976 were made with Hanford Engineering Development Laboratory, Lawrence Livermore Laboratory, Battelle Northwest Laboratory, Oak Ridge National Laboratory, CEN/SCK Laboratory (Mol, Belgium) and the University of Washington (Seattle). The five "spike" systems used to dispense exactly-known quantities of ^{3}He and/or ^{4}He to the helium

released by solid samples were refilled. Cross checks using various combinations of spikes showed excellent intercalibration agreement.

A considerable amount of effort was expended in maintaining vacuum valves worn from years of use. Replacements for these, and a high sensitivity amplifier requested from Capital Equipments funds for FY 1976 have again been listed in the FY 1977 189a forms. An automated set of valves in the sample purification line will provide greater operational reliability and analysis reproducibility.

H. PUBLICATIONS

1. "Dosimetry for Fluence Applications," by Harry Farrar IV, E. P. Lippincott, and W. N. McElroy, Proceedings of the 1st ASTM-EURATOM Symposium on Reactor Dosimetry, Petten, The Netherlands, September 1975.

2. "Helium Profiles Across Fast Reactor Fuel Pin Cladding," by Harry Farrar IV, C. W. Hunter, G. D. Johnson, and E. P. Lippincott, presented at the ANS 1976 Annual Meeting, Toronto, June 15, 1976. Published in the Conference Transactions: (Trans. Am. Nucl. Soc. 23 156 (1976)).

3. "Helium Charging of Metals by Tritium Decay" by J. F. Remark, A. B. Johnson, Jr., Harry Farrar IV, and D. G. Atteridge, Nucl. Technol. 29 369 (1976).

4. "Helium Production in Reactor Materials," by E. P. Lippincott, W. N. McElroy and H. Farrar IV, in Nuclear Cross Sections and Technology, Vol. I, pp 375-377, R. A. Schrack and C. D. Bowman, Eds., NBS Special Publication 425, U.S. Department of Commerce, October 1975.